AJNR

Gray Matter n-Acetyl Aspartate Deficits in Secondary Progressive but Not Relapsing-Remitting Multiple Sclerosis

Elfar Adalsteinsson, Annette Langer-Gould, Ronald J. Homer, Archana Rao, Edith V. Sullivan, Christiane Abbehusen Lima, Adolf Pfefferbaum and Scott W. Atlas

AJNR Am J Neuroradiol 2003, 24 (10) 1941-1945
http://www.ajnr.org/content/24/10/1941

AJNR Am J Neuroradiol 24:1941–1945, November/December 2003

Gray Matter N-Acetyl Aspartate Deficits in Secondary Progressive but Not Relapsing-Remitting Multiple Sclerosis

Elfar Adalsteinsson, Annette Langer-Gould, Ronald J. Homer, Archana Rao, Edith V. Sullivan, Christiane Abbehusen Lima, Adolf Pfefferbaum, and Scott W. Atlas

BACKGROUND AND PURPOSE: **Spectroscopic examination of multiple sclerosis (MS) patients has revealed abnormally low N-acetyl-aspartate (NAA) signal intensity, even in brain tissue that appears normal on high-resolution structural MR images but has yielded inconclusive evidence to distinguish the well-documented clinical differences between MS subtypes. This study used proton MR spectroscopic imaging (MRSI) and high-resolution MR imaging to characterize metabolite profiles in normal-appearing brain tissue of relapsing-remitting multiple sclerosis (RRMS) and secondary progressive (SP) MS.**

METHODS: **Volumetric spiral MRSI was used together with high-resolution MR imaging to derive absolute measures of metabolite concentrations separately in normal-appearing supratentorial cerebral gray matter and white matter in five RRMS patients, five SPMS patients, and nine age-matched controls. Structural MR images were segmented into compartments of gray matter, white matter, CSF, and lesions, and metabolite signals per unit of tissue volume were calculated for gray matter and white matter separately.**

RESULTS: **Only the SPMS group had significantly lower NAA concentrations in normal-appearing gray matter compared with concentrations in controls. NAA in normal-appearing white matter was equally reduced in RRMS and SPMS patients. The functional relevance of this brain metabolite measure was suggested by the observed but statistically nonsignificant correlation between higher disability scores on the Expanded Disability Status Scale and lower gray matter NAA concentrations.**

CONCLUSION: **The otherwise occult abnormality in supratentorial gray matter in SPMS but not RRMS may explain the more severe physical and cognitive impairments afflicting patients with SPMS that do not correlate well with visible lesion burden.**

Multiple sclerosis (MS) is a neurodegenerative disease with characteristic lesions in brain white matter. As a progressive disorder, MS-related symptoms worsen with time, but the course of functional decline can vary across patients (1). More than 80% of patients with MS begin with a relapsing-remitting form of the illness (RRMS); however, 5–20 years after disease onset, most RRMS patients enter the progressive phase of disease, called secondary progressive MS (SPMS). This progressive phase is marked by unrelenting physical and cognitive decline, implicating neuronal damage. A small percentage of patients follows a primary progressive course, marked by a continuous, unremitting decline from symptom onset (2). Presently, there are no reliable tests to predict who of the RRMS type will develop SPMS and when they will develop it. Similarly, determination of when transition from the relapsing-remitting phase to the progressive phase occurs can be accomplished only retrospectively. A quantitative test that could accurately classify or predict MS clinical subtypes could make a significant contribution to patient management decisions and provide an outcome measure in MS clinical trials.

Potential markers for distinguishing MS stage and

Received May 13, 2003; accepted after revision July 2.

From the Departments of Radiology (E.A., R.J.H., A.R., C.A.L., S.W.A.), Neurology (A.L.-G.), and Psychiatry and Behavioral Sciences (E.V.S., A.P.), Stanford University School of Medicine, Stanford, CA, and the Neuroscience Program (A.P.), SRI International, Menlo Park, CA.

Supported in part by the National Institutes of Health (grants AG18942, RR09784, AA12388, AA12999, NS39319, and NS43207) and a Wadsworth Foundation Young Investigator's Award. Parts of this work were presented at the annual meeting of the International Society for Magnetic Resonance in Medicine, Toronto, Canada, July 10–16, 2003.

Address correspondence to Elfar Adalsteinsson, PhD, Department of Radiology, Stanford University School of Medicine, Stanford, CA 94305.

severity would require in vivo quantification of brain gray matter and white matter integrity. The recent inclusion of T2-weighted MR imaging information as a diagnostic criterion has significantly improved diagnostic specificity and has hastened diagnostic determination in MS (3). In vivo proton MR spectroscopic imaging (MRSI) allows examination of brain tissue integrity on a biochemical level and may be sensitive to subtle changes initially occurring at that level.

Of particular importance to the study of neurodegenerative conditions is N-acetylaspartate (NAA). The N-acetyl peak comprises several N-acetylated compounds including NAA, which is present only in living, mature neurons and not glia (4, 5). When the amount of underlying gray matter is taken into account by expressing NAA per unit volume of gray matter, such NAA gray matter concentration does not decline in healthy aging (6) but does so in degenerative diseases, including Alzheimer disease (AD) (7). MRSI has been useful in detecting gray matter NAA concentration decline longitudinally in AD patients occurring at the same rate of decline as observed in global cognitive functioning (8). These studies provide in vivo validation of tissue-specific MRSI quantification of NAA in gray matter as a selective marker of neuronal degradation.

Spectroscopic examination of MS patients has revealed abnormally low NAA signal intensity, even in brain tissue that appears normal on high-resolution structural MR images. Single-voxel and single-section studies have shown that samples of small areas of normal-appearing tissue that are mostly gray matter can be spectroscopically abnormal in MS (9–11). Single-spectrum, whole-brain MRS studies report significant NAA deficits that precede lesion detection with conventional MR imaging (12–14). Because NAA is present primarily, if not exclusively, in neurons (5, 15), the NAA deficit in MS has been interpreted as reflecting neuronal degeneration, possibly resulting from demyelination or Wallerian degeneration.

In the present study, we used volumetric MRSI combined with segmented, high-resolution MR imaging for tissue classification to test whether SPMS patients would have greater or more widespread deficits than RRMS patients in NAA concentrations of normal-appearing gray matter or white matter and whether the extent of metabolite abnormality correlates with functional status. Group differences in specific metabolite concentrations and tissue types could provide clues to neural mechanisms underlying symptomatic differences in the MS course.

Methods

Participants

The subject groups included five RRMS patients (all women), five SPMS patients (one man, four women), and nine controls (one man, eight women). Each patient met Poser criteria (16) for clinically definite multiple sclerosis. Transition to SPMS was defined as prior RRMS course followed by continual worsening of symptoms and signs for a period of at least 6 months, with or without superimposed relapses (17). As expected, disease duration was longer in SPMS (mean = 19.4 ± 3.72 years) than in RRMS (mean = 8.2 ± 6.26 years) patients ($Z = 2.2$; $P < .03$).

Demographic and clinical characteristics of each MS patient

Diagnosis	Sex	EDSS	Age (years)	Disease Duration (years)	Medication
RRMS	Female	3.0	38	6	Beta interferon
RRMS	Female	2.0	44	4	Glatiramer acetate
RRMS	Female	3.5	23	8	Beta interferon
RRMS	Female	3.0	46	19	Beta interferon
RRMS	Female	2.0	28	4	Beta interferon
SPMS	Female	6.5	39	21	Glatiramer acetate
SPMS	Female	8.0	64	20	None
SPMS	Female	8.0	53	24	Beta interferon
SPMS	Female	6.5	46	14	Beta interferon
SPMS	Male	4.0	42	18	Beta interferon

Note.—EDSS, Expanded Disability Status Scale; RRMS, relapsing-remitting multiple sclerosis; SPMS, secondary progressive multiple sclerosis.

The groups did not differ significantly in age (RRMS = 35.9 ± 9.8 years; SPMS = 48.8 ± 9.9 years; controls = 41.1 ± 13.8 years) (F [2, 19] = 1.58 [n.s.]). The Table presents relevant demographic and clinical data for each patient. This research was approved by the local institutional review board, and all subjects gave written informed consent before participation.

Imaging Protocol

All subjects were imaged with commercially available MR imaging equipment (1.5 T; General Electric Corporation, Milwaukee, WI) with a standard quadrature head coil. The MR system was equipped with echo-speed gradients capable of 4 G/cm maximum gradient amplitude and 150 T/m/s slew rate. The acquisition protocol included a sagittal localizer followed by axial dual-echo fast spin-echo ([FSE] TE = 15/90 ms, TR = 4 s) and fluid-attenuated inversion recovery ([FLAIR] TE = 113 ms, TR = 9 s, TI = 2250 ms) sequences, both with 18 contiguous sections, 7 mm thick, 256 × 192 pixels across a 24-cm field of view (FOV).

Before MRSI, the main field homogeneity was optimized over the supratentorial brain by adjusting the linear and nonlinear shim terms on the MR system. The shim volume was drawn on a graphical user interface, and updated shim currents were calculated from a 32-section spiral field map acquisition (18), which took 4 s to acquire.

Metabolite data were acquired in the axial plane covering the supratentorial brain with a volumetric, variable-density spiral MRSI with 1.2-mL spatial resolution (19). Subject to gradient slew rate and amplitude constraints, the sampling density of the spiral trajectories was designed to match a Hanning window. The maximum spiral diameter in (k_x,k_y) was 36 pixels, with 32 phase encodes in k_z to sample an ellipsoid in (k_x,k_y,k_z)-space. The in-plane FOV was 24 cm, whereas through-plane FOV was 11.2 cm. The reconstructed spectral bandwidth was 400 Hz, and the readout period was 232 ms. Acquisition time was 15 minutes 20 seconds. A 3D gridding reconstruction was used to resample the nonuniformly sampled data onto a Cartesian grid before a 4D fast Fourier transform.

A spin-echo, spectral-spatial excitation suppressed the water signal intensity while exciting the resonances of NAA, creatine and phosphocreatine (Cr), and choline-containing compounds (Cho). Inversion recovery preceded the excitation for improved lipid suppression (TI/TE/TR = 170 ms/144 ms/2 s). A separate 9-minute acquisition was used to acquire a reference signal intensity from the unsuppressed water with a reduced repetition period (TR = 1.2 s). The high signal-to-noise ratio (SNR)

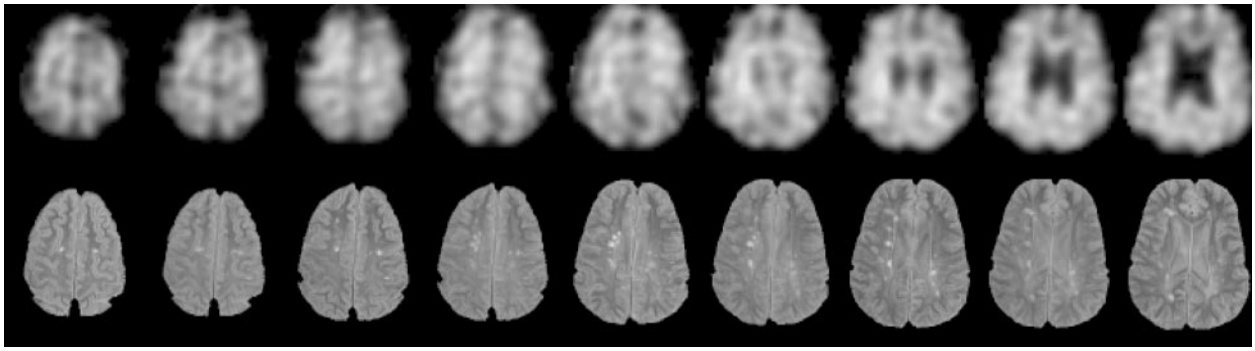

FIG 1. Example of nine axial sections used in quantification of metabolites (NAA images, *top*) and lesions (FLAIR images, *bottom*).

water reference data were used for phasing and main-field inhomogeneity corrections and to aid in the quantification of metabolite signals. An image of the unsuppressed water and a field map were produced from the reference signal intensity and applied in subsequent processing. Three separate metabolite images for NAA, Cr, and Cho were produced by a least squares fit to the phased metabolite spectrum for each voxel. Corrections for receiver gain and coil loading were made to allow comparisons of absolute metabolite signal intensity levels among subjects.

Image Analysis

The FSE and FLAIR images were stripped of extra-brain tissue and automatically segmented into compartments of gray matter, white matter, CSF, and focal signal intensity hyperintensities on FLAIR images. This processing was run with software tools developed in house according to the following outline. The stripping of extra-brain tissue is based on the late-echo FSE data, which provide high contrast between sulcal CSF and skull. The CSF compartment was estimated with a nonparametric histogram operator (20) on the basis of data synthesized as the difference between the early and late-echo FSE. The CSF was removed from the FLAIR images, and hyperintensities were considered signal higher than a threshold value on the non-CSF FLAIR tissue map. The chosen threshold was the mean signal intensity plus 2.5 times the standard deviation of the FLAIR tissue. Gray and white matter were segmented on the basis of data synthesized as the sum of the early- and late-echo FSE. A 2D homomorphic filter (21) with a 31-mm extent was used to remove slow intensity variations such as those arising from inhomogeneity of the excitation field, followed by a nonparametric histogram operator (20) to separate the gray and white matter tissue compartments.

The structural data were aligned with the spectroscopic water reference images, and the aligned, segmented data were filtered by the same *k*-space sampling and window parameters as were applied to the spiral MRSI data to create low-resolution tissue maps to match the metabolite images. For a given spectroscopic voxel, the signal intensity contribution from each tissue type is proportional to the value given by the filtered maps. Thus, the filtered tissue maps were combined with the metabolite images and used to solve for metabolite signal intensity levels in compartments of gray matter, white matter, and the entire analyzed region (Fig 1) (6).

The quantified region subtended a 31.5-mm-thick axial slab, centered at the FSE section immediately superior to the lateral ventricles. Voxels that deviated by more than ±10 Hz in main field homogeneity were excluded from analysis based on a field map derived from the water reference acquisition. This volume was chosen to maximize the number of included voxels while avoiding regions that suffer from signal intensity loss and artifacts from main field inhomogeneities near air-tissue interfaces. The unit of measure was the metabolite signal intensity level per unit tissue volume and was calculated for total tissue (gray matter plus white matter plus lesions) and then separately in gray matter and white matter, exclusive of lesions.

Statistical Analysis

Group differences in metabolite concentrations and tissue volumes were tested with one-way and repeated-measures analysis of variance (ANOVA); follow-up group comparisons were made with *t* tests (two-tailed alpha = 0.05). Function was measured with the Expanded Disability Status Scale (EDSS), an ordinal measure where higher scores indicate greater physical impairment (22). The EDSS data were subjected to nonparametric analysis; Mann-Whitney tests examined group differences, and relationships between MRSI measures and EDSS scores were tested with Spearman rank correlations.

Results

The three groups did not differ significantly in volume of gray matter (F [2, 18] = 1.77; P = .21) or white matter (F [2, 18] = 1.57; P = .24) within the MRSI-quantified brain region. Further, within the same region, the RRMS and SPMS groups did not differ significantly in volume of lesion load measured on FLAIR images (t [8] = 0.97; P = .36). In contrast to the MR imaging structural data, one-way, three-group ANOVA yielded significant group effects for total tissue (normal plus abnormal, gray matter plus white matter) concentration of NAA (F [2, 18] = 9.56; $P < .002$). Follow-up tests indicated that both MS groups had significantly lower total tissue NAA concentrations than those in controls but the two MS groups did not differ from each other. The groups did not differ in total tissue concentration of either Cr (F [2, 18] = 1.55; P = .24) or Cho (F [2, 18] = 0.465; P = .63). The group differences were confirmed with nonparametric analysis.

A three-group repeated measures ANOVA comparing NAA in nonlesion white matter and gray matter revealed a significant group effect (F [2, 16] = 6.64; $P < .008$) and a trend toward a group by tissue type interaction (F [2, 16] = 2.72; $P < .10$). Follow-up analyses indicated that both the RRMS and SPMS groups had significantly lower nonlesion white matter NAA concentrations than controls. By contrast, only the SPMS group exhibited a significant normal-appearing gray matter NAA concentration deficit. This effect was confirmed by a two-group (RRMS versus SPMS) repeated-measures ANOVA, which yielded a two group by two tissue type interaction: F (1, 8) =

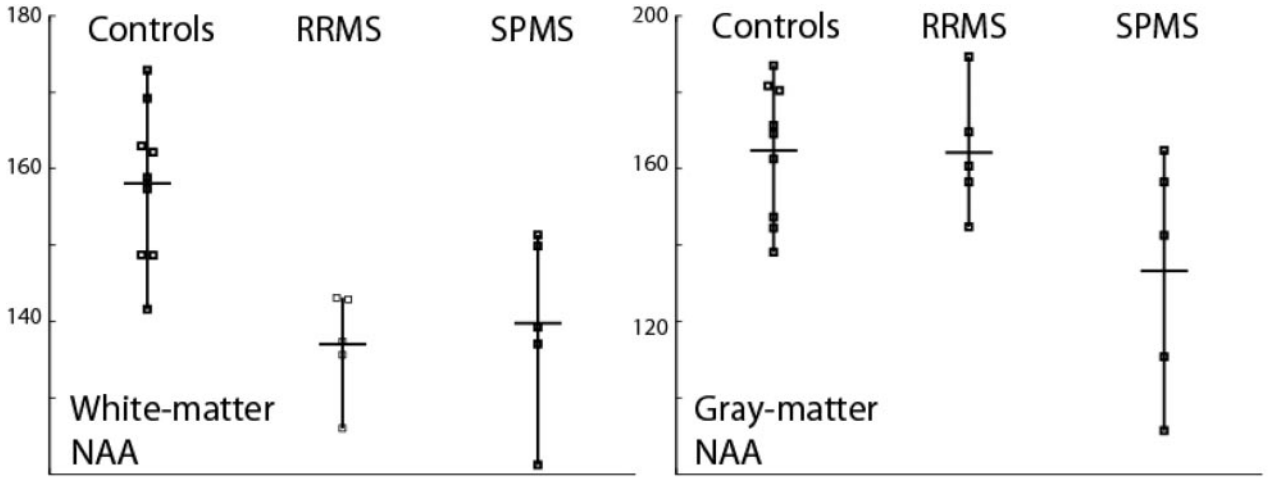

FIG 2. Group means and individual data of NAA concentrations in GM and WM in controls, RRMS, and SPMS.

5.59; $P < .05$ (Fig 2). Of interest, one SPMS patient had severe clinical disease of long duration but minimal supratentorial lesion load; she also had the highest NAA gray concentration of the SPMS group, which was at the mean level of the RRMS and control groups.

As expected, the SPMS group (range = 4.0 to 8.0) was significantly more impaired than the RRMS group (range = 2.0 to 3.5; $Z = 2.64$, $P < .01$). Higher EDSS scores were not significantly correlated with lower gray matter NAA concentrations ($\rho = -.53$; $P < .06$, one tailed).

Discussion

The results of this analysis revealed two different patterns of biochemical abnormality in brain tissue that appeared normal on FLAIR images in MS: significant NAA deficits were present in both gray matter and white matter of SPMS patients, whereas gray matter NAA deficits were present only in RRMS patients. These patterns of NAA deficits occurred despite absence of MS group differences in gray matter or white matter volumes and were more sensitive in these small groups than supratentorial lesion load based on automated quantitation of FLAIR images.

There are several limitations of this study, including the low number of subjects in each group. The inability to detect a difference in lesion load on FLAIR images may be related to the small sample size. As is clear from Figure 2, there is overlap between the RRMS and SPMS groups in gray matter NAA concentrations, so this technique cannot be applied, as currently implemented, to individual cases to separate subtypes of MS. Several sources could contribute to the variance of the NAA metric, including low SNR in MRSI at 1.5 T, uncertainty in segmentation of lesions and tissue types arising from the relatively thick structural imaging sections (7 mm), as well as true physiologic variability among individuals with MS. The variance of the gray matter NAA marker due to low metabolite SNR can be reduced by imaging at higher fields, such as 3 T, as well as by the application of multichannel receiver coils for neuroimaging. The segmentation can be improved by incorporating higher resolution structural imaging into the protocol, with thinner sections for the T2-weighted data as well as volumetric T1-weighted images. With the improved acquisition methods, a better understanding of the underlying physiologic variations can be obtained.

Prior studies have successfully used MRSI to identify biochemical abnormalities in brain but most have focused on white matter with lesions (23) and normal-appearing white matter (24, 25). A combined in vivo and biopsy analysis indicated that in MS the NAA peak reflects neuronal and axonal integrity (26). The relevance of gray matter in MS disability was emphasized by studies based on FDG positron emission tomography, which showed cerebral metabolic rate of glucose in gray matter was significantly lower in MS than in controls (27–29). The few studies that have investigated the biochemical integrity of cortical gray matter have not made absolute measurements of metabolites in separate gray matter and white matter compartments or have had limited coverage (9, 25, 30, 31). In a 30-month longitudinal study, DeStefano et al (32) examined a large sample of central white matter of RRMS patients and observed a relationship between fluctuations of NAA/Cr ratios and EDSS during periods of clinical relapse and remission. In another study, Pan et al (33) acquired single-section MRSI data at 4.1 T that extended to the cortical regions. Metabolite ratios of Cr/NAA in gray matter voxels were modestly greater in MS than in controls and Cho/NAA and Cr/NAA were elevated in periventricular voxels. Single-spectrum, whole-brain NAA measurements that do not resolve metabolite information spatially have also been applied to study MS (12–14) but by their nature cannot be used to resolve metabolite profiles from different tissue compartments within the brain. The MRSI findings of the present study comport with those of the previous MRSI studies and add to speculations implicating gray matter in addition to white matter degradation

with disease progression and as underlying NAA deficits in MS.

Conclusion

The difference in metabolite pattern in normal-appearing gray matter versus white matter NAA may explain the more severe physical and cognitive impairments afflicting patients with SPMS relative to those with RRMS (34). As a safe and noninvasive technique, quantitative gray matter NAA measurements in serial volumetric MRSI may be an effective way to distinguish RRMS from early SPMS patients both before and after treatment.

Acknowledgments

We thank Allison Pearl for help with image acquisition.

References

1. Confavreux C, Vukusic S, Moreau T, Adeleine P. **Relapses and progression of disability in multiple sclerosis.** *N Engl J Med* 2000; 343:1430–1438
2. McDonald WI. **Relapse, remission, and progression in multiple sclerosis [editorial].** *N Engl J Med* 2000;343:1486–1487
3. Dalton CM, Brex PA, Miszkiel KA, et al. **Application of the new McDonald criteria to patients with clinically isolated syndromes suggestive of multiple sclerosis.** *Ann Neurol* 2002;52:47–53
4. Tallan HH. **Studies on the distribution of N-acetyl-L-aspartate acid in brain.** *J Biol Chem* 1956;224:41–45
5. Petroff OAC, Pleban LA, Spencer DD. **Symbiosis between in vivo and in vitro NMR spectroscopy: the creatine, N-acetylaspartate, glutamate and GABA content of the epileptic human brain.** *Magn Reson Imaging* 1995;13:1197–1211
6. Pfefferbaum A, Adalsteinsson E, Spielman D, et al. **In vivo spectroscopic quantification of the N-acetyl moiety, creatine and choline from large volumes of gray and white matter: effects of normal aging.** *Magn Reson Med* 1999;41:276–284
7. Pfefferbaum A, Adalsteinsson E, Spielman D, et al. **In vivo brain concentrations of N-acetyl compounds, creatine and choline in Alzheimer's disease.** *Arch Gen Psychiatry* 1999;56:185–192
8. Adalsteinsson E, Sullivan EV, Kleinhans N, et al. **Longitudinal decline of the neuronal marker N-acetyl aspartate in Alzheimer's disease.** *Lancet* 2000;355:1696–1697
9. Chard DT, Griffin CM, McLean MA, et al. **Brain metabolite changes in cortical grey and normal-appearing white matter in clinically early relapsing-remitting multiple sclerosis.** *Brain* 2002; 125:2342–2352
10. Cifelli A, Arridge M, Jezzard P, et al. **Thalamic neurodegeneration in multiple sclerosis.** *Ann Neurol* 2002;52:650–653
11. Sarchielli P, Presciutti O, Tarducci R, et al. **Localized (1)H magnetic resonance spectroscopy in mainly cortical gray matter of patients with multiple sclerosis.** *J Neurol* 2002;249:902–910
12. Filippi M, Bozzali M, Rovaris M, et al. **Evidence for widespread axonal damage at the earliest clinical stage of multiple sclerosis.** *Brain* 2003;126:433–437
13. Gonen O, Catalaa I, Babb JS, et al. **Total brain N-acetylaspartate: a new measure of disease load in MS.** *Neurology* 2000;54:15–19
14. Gonen O, Moriarty DM, Li BS, et al. **Relapsing-remitting multiple sclerosis and whole-brain N-acetylaspartate measurement: evidence for different clinical cohorts initial observations.** *Radiology* 2002;225:261–268
15. Griffin JL, Bollard M, Nicholson JK, Bhakoo K. **Spectral profiles of cultured neuronal and glial cells derived from HRMAS (1)H NMR spectroscopy.** *NMR Biomed* 2002;15:375–384
16. Poser CM, Paty DW, Scheinberg L, et al. **New diagnostic criteria for multiple sclerosis: guidelines for research protocols.** *Ann Neurol* 1983;13:227–231
17. Schumacher GA, Beebe G, Kibler RF, et al. **Problems of experimental trials of therapy in multiple sclerosis: report by the Panel on the Evaluation of Experimental Trials of Therapy in Multiple Sclerosis.** *Ann N Y Acad Sci* 1965;122:552–568
18. Kim DH, Adalsteinsson E, Glover GH, Spielman DM. **Regularized higher-order in vivo shimming.** *Magn Reson Med* 2002;48:715–722
19. Adalsteinsson E, StarLack J, Meyer C, Spielman D. **Reduced spatial side lobes in chemical-shift imaging.** *Magn Reson Med* 1999; 42:314–323
20. Otsu N. **A threshold selection method from gray-level histograms.** *IEEE Trans Syst Man Cybern* 1979;9:63–66
21. Lim KO, Pfefferbaum A. **Segmentation of MR brain images into cerebrospinal fluid spaces, white and gray matter.** *J Comput Assist Tomogr* 1989;13:588–593
22. Kurtzke JF. **Rating neurologic impairment in multiple sclerosis: an expanded disability status scale (EDSS).** *Neurology* 1983;33:1444–1452
23. Hirsch JA, Lenkinski RE, Grossman RI. **MR spectroscopy in the evaluation of enhancing lesions in the brain in multiple sclerosis.** *Am J Neuroradiol* 1996;17:1829–1836
24. Davie CA, Barker GJ, Thompson AJ, et al. **1H magnetic resonance spectroscopy of chronic cerebral white matter lesions and normal appearing white matter in multiple sclerosis.** *J Neurol Neurosurg Psychiatry* 1997;63:736–742
25. Narayanan S, Fu L, Pioro E, et al. **Imaging of axonal damage in multiple sclerosis: spatial distribution of magnetic resonance imaging lesions.** *Ann Neurol* 1997;41:385–391
26. Bitsch A, Bruhn H, Vougioukas V, et al. **Inflammatory CNS demyelination: histopathologic correlation with in vivo quantitative proton MR spectroscopy.** *Am J Neuroradiol* 1999;20:1619–1627
27. Schiepers C, Van Hecke P, Vandenberghe R, et al. **Positron emission tomography, magnetic resonance imaging and proton NMR spectroscopy of white matter in multiple sclerosis.** *Mult Scler* 1997; 3:8–17
28. Blinkenberg M, Bonde C, Holm S, et al. **Rate dependence of regional cerebral activation during performance of a repetitive motor task: a PET study.** *J Cer Blood Flow Metab* 1996;16:794–803
29. Bakshi R, Miletich RS, Kinkel PR, et al. **High-resolution fluorodeoxyglucose positron emission tomography shows both global and regional cerebral hypometabolism in multiple sclerosis.** *J Neuroimaging* 1998;8:228–234
30. Rooney WD, Goodkin DE, Schuff N, et al. **1H MRSI of normal appearing white matter in multiple sclerosis.** *Mult Scler* 1997;3: 231–237
31. Husted C, Goodin D, Hugg J, et al. **Biochemical alterations in multiple sclerosis lesions and normal-appearing white matter detected by in vivo 31P and 1H spectroscopic imaging.** *Ann Neurol* 1994;36:157–165
32. De Stefano N, Matthews PM, Fu L, et al. **Axonal damage correlates with disability in patients with relapsing- remitting multiple sclerosis: results of a longitudinal magnetic resonance spectroscopy study.** *Brain* 1998;121:1469–1477
33. Pan JW, Hetherington HP, Vaughan JT, et al. **Evaluation of multiple sclerosis by 1H spectroscopic imaging at 4.1 T.** *Magn Reson Med* 1996;36:72–77
34. Nusbaum AO, Tang CY, Wei T, et al. **Whole-brain diffusion MR histograms differ between MS subtypes.** *Neurology* 2000;54:1421–1427